

# CALCULATION OF PRESSURE DROPS THROUGH ATUCHA-II FUEL ASSEMBLY SPACER GRIDS

D. Melideo<sup>1</sup>, F. Moretti<sup>1</sup>, F. Terzuoli<sup>1</sup>, F. D'Auria<sup>1</sup>, O. Mazzantini<sup>2</sup>

<sup>1</sup> University of Pisa, <sup>2</sup> Nucleoeléctrica Argentina S.A.

## Abstract

A commercial CFD code was applied, for validation purposes, to the simulation of the spacer grid of Atucha-II coolant channel. The calculations were aimed at evaluating the pressure drop across the grid during the normal operation. Two types of grid were simulated, i.e. the so-called “elastic spacer” and “rigid spacer”, which are made from different materials and have totally different geometries. Both designs are planned to be adopted in Atucha-II reactor.

The numerical results were compared with the measured data obtained from experiments performed at the High Pressure Test Laboratory in the Atomic Centre “Ezeiza”, in Argentina. The spacer grids used for the experiments are exact replicas of those to be installed at Atucha-II. According to the Best Practice Guidelines recommendations, several calculations were performed to investigate the sensitivity of the results to the turbulence model, the advection scheme, the working fluid, etc. The results for the elastic spacer grid are in good agreement with the experimental values. The results for the rigid grid show a considerable sensitivity to the advection scheme; it appears that the first-order Upwind advection scheme yields better results than the higher resolution scheme available in the code.

## 1 INTRODUCTION

The aim of this work is to evaluate the pressure drop across the grid during the normal operation, and to qualify the CFD model for this kind of application. Two types of grid are being considered for utilization in Atucha-II reactor, i.e. the so-called “elastic spacer” and “rigid spacer” (also referred to as the KWU and IEC spacer, respectively), which are made from different materials and have totally different geometries. Both designs were simulated. The KWU spacer is constituted by bended plates, while the IEC spacer is obtained from a single metal sheet cut with high-pressure water jet. Both designs also include four rigid sliding shoes welded to the spacers and an elastic shoe connected to the spacers too. The sliding shoes serve as radial constraints between the fuel bundle and the coolant channel.

The CFD code adopted for the simulation is ANSYS CFX 11.0. The meshes have been created with ANSYS ICEM 11.0. The obtained results have been compared with the experimental data found in a report provided by NA-SA [1] Furthermore, several sensitivity calculations have been performed in order to apply Best Practice Guidelines recommendations [2].

## 2 SPACER GRIDS

### 2.1 The elastic spacer design (KWU)

The elastic spacer (Figure 1) is constituted by bended plates. Four rigid sliding shoes are welded to the spacer; an elastic shoe is connected to the spacer too. The thickness of the spacer is 0.48 mm, except for the thickness of the external ring which is 0.75 mm. The total height of the spacer is 32 mm. The fuel rod clad is in direct contact with the spacer. The flow area of the coolant channel without accounting for the spacer can be calculated as follows:

$$A_{NO\ GRID} = \pi \cdot (d_{CC}^2 - 37 \cdot d_{FR}^2) / 4 \quad (1)$$

Imposing that the coolant channel diameter ( $d_{CC}$ ) and the fuel rod diameter ( $d_{FR}$ ) are 0.1082 m and 0.0129 m respectively, the resulting flow area is  $0.004359 \text{ m}^2$ . In presence of the grid, the flow area is reduced by the area of the spacer (i.e.  $0.001422 \text{ m}^2$ ). Consequently the resulting flow area ratio is 0.674.

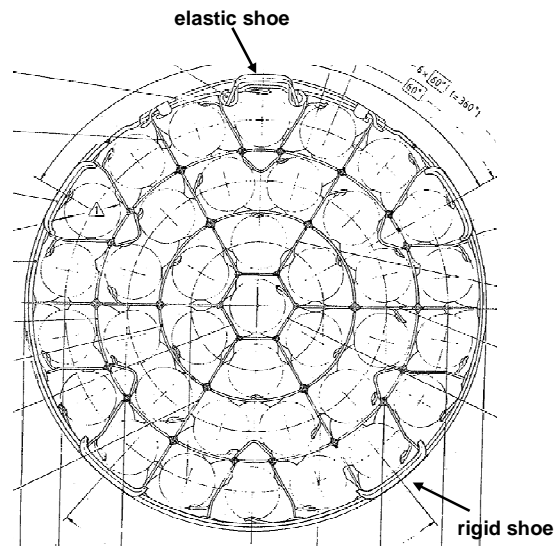


Figure 1. The elastic spacer design (KWU)

### 1.1 The rigid spacer design (IEC)

The rigid spacer (see Figure 2) is fabricated from a 34 mm metal sheet from which the material is cut with a high-pressure water jet. Four rigid sliding shoes are then welded to the spacer; an elastic shoe is connected to the spacer too. The thickness of the spacer in regular zones is 0.8 mm; thickness is larger in those locations where the fuel rods are supported (three per rod). Some holes are drilled on large-thickness regions.

The fuel rod clad do not directly touch the spacer; rather, metal parts (called “*patines*” in NA-SA drawings) welded on the rods clad are in direct contact with the spacer.

The flow area of the coolant channel without accounting for the rigid spacer is the same of the elastic spacer calculated (i.e.  $0.004359 \text{ m}^2$ ). The resulting flow area ratio for the IEC design is 0.578.

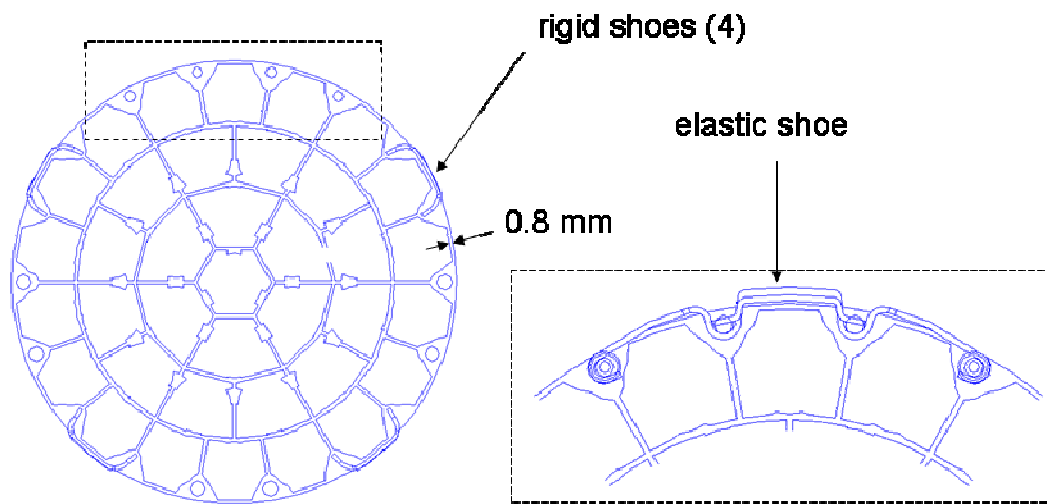


Figure 2. The rigid spacer design (IEC)

### 3 EXPERIMENTAL DATA

The experiments were performed at the “Laboratorio de Ensayos de Alta Presión” (LENAP) in the “Centro Atómico Ezeiza” (CAE). The grid used for the experiments are both the IEC and the KWU spacer grid (i.e. similar to the ones installed at Atucha-II NPP). The scheme of the facility is reported in Figure 3.

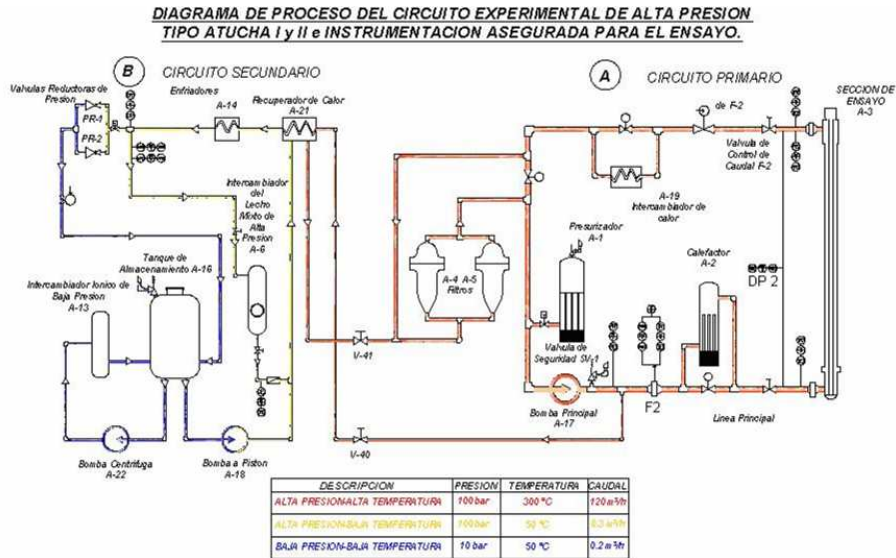


Figure 3. Scheme of the experimental facility

The experiments were performed in order to evaluate the pressure drop along the coolant channel due to the presence of the spacer grids; the number of spacer grid inside the coolant channel was 15. Several tests have been performed using the heavy water at the constant pressure of 80 bar, at different temperatures (from 100° C to 250° C) and at different mass flows (from 4 kg/s to 31 kg/s). In Figure 4 and in Figure 5 the experimental values (i.e. the measured pressure drops) for different mass flow rates are reported for KWU and IEC spacer grids, respectively. The pressure drop is calculated between the inlet and the outlet of the fuel channel.

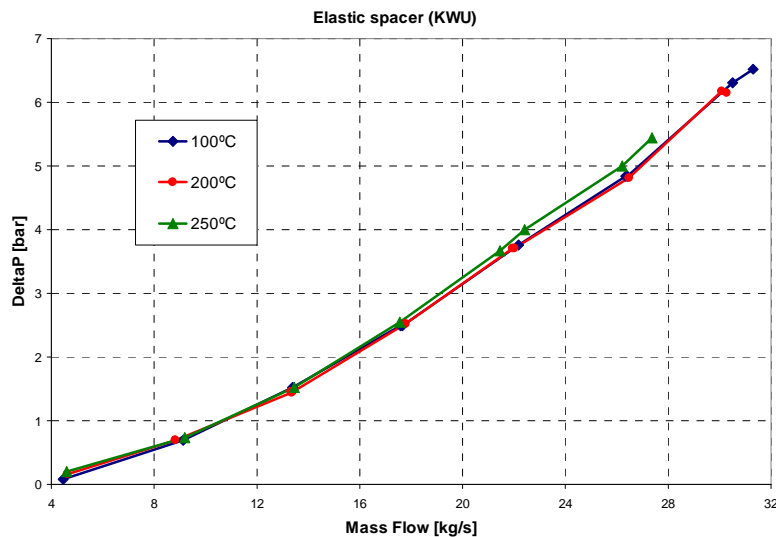


Figure 4. Experimental value for KWU spacer grid

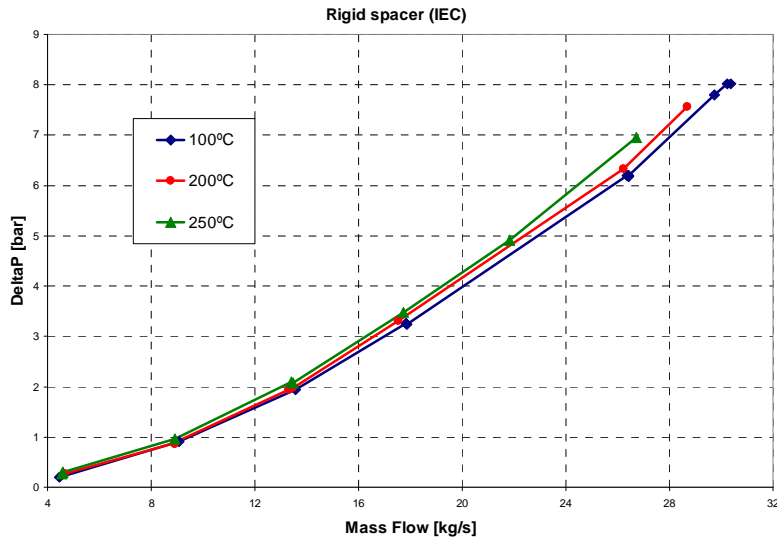


Figure 5. Experimental value for IEC spacer grid

In order to compare the experimental data with the CFD results two cases have been chosen, one for the KWU spacer grid and the other for the IEC spacer grid (Table 1)

	<b>KWU</b>	<b>IEC</b>
Temperature [°C]	250	250
Mass flow rate [kg/s]	26.22	26.71
Number of spacers	15	15
DeltaP [bar]	5.001	6.95
Area [m <sup>2</sup> ]	0.004359	0.004359
Density [kg/m <sup>3</sup> ] (HW)	884.6	884.6
Delta P for 1 spacer [Pa]	33340.0	46333.3

Table 1 – Experimental value chosen for the comparison with the CFD results

The CFD results reported in this paper are in terms of pressure loss coefficient related to one single spacer. The pressure loss coefficient is calculated from the following formula:

$$K = \frac{2 \cdot \Delta p}{\rho \cdot \bar{v}^2} = \frac{2 \cdot \Delta p \cdot \rho \cdot A^2}{\dot{m}^2} \quad (2)$$

where  $\Delta p$  is the pressure difference between inlet and outlet boundaries,  $\rho$  is the density ( $\rho = 884.6 \text{ kg/m}^3$  at  $250^\circ\text{C}$ ),  $\bar{v}$  is the average velocity,  $A$  is the coolant channel flow area.

Using the Equation 2, the experimental pressure loss coefficient values for the two types of grid are those reported in Table 2.

	<b>KWU</b>	<b>IEC</b>
K (HW)	1.63	2.18

Table 2 – Experimental value used for the comparison with the CFD results

## 4 CFD SIMULATIONS

### 4.1 Computational domain for KWU spacer grid

The computational domain for the mesh of the KWU spacer is constituted by 1/6 of the whole domain; in particular, the sector including the elastic shoe has been chosen (see Figure 6). The axial length of the domain is 0.445 m (i.e. the distance between two adjacent spacers) and the smallest geometrical details have been considered. The computational domain used to create the mesh includes the coolant channel wall, the fuel rod wall the elastic shoe and the rigid spacer wall.

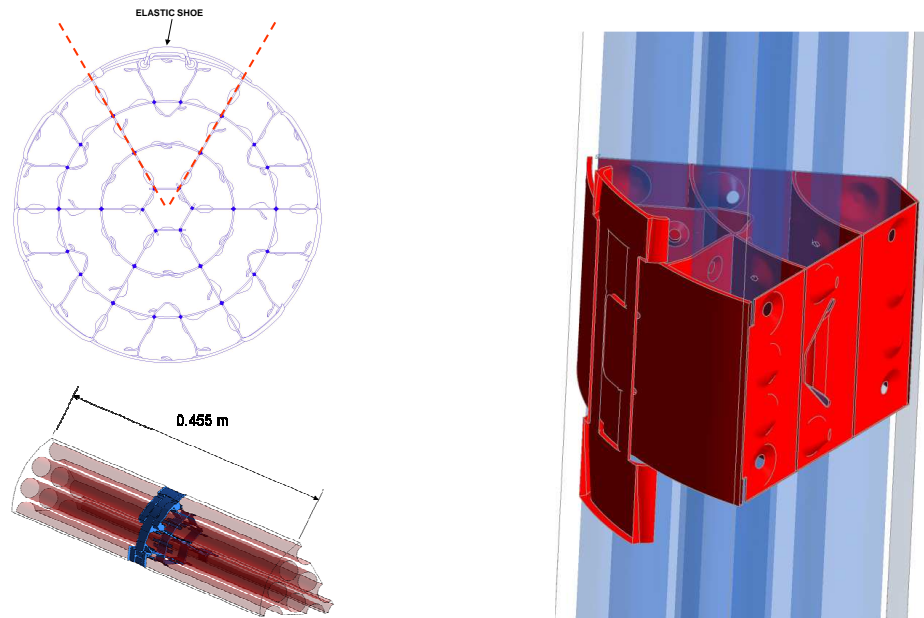


Figure 6. KWU computational domain

### 4.2 Computational domain for IEC spacer grid

As for the KWU spacer the computational domain is 0.455 m long and includes one single spacer, as shown in Figure 7. Moreover, the domain is reduced to one 60° sector (e.g. the three sectors in the figure). Sector 1 is affected by the presence of the elastic shoe, and is expected to yield the largest flow resistance. A lower flow resistance is expected in Sector 2 and in Sector 3.

The left side is symmetric to the right side. The position of the spacer with respect to the coolant channel is not exactly coaxial, due to the presence of just one elastic shoe. The eccentricity is around 0.3 mm and is taken into account in the CFD model.

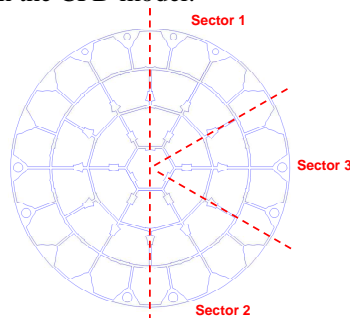


Figure 7. IEC computational grid

### 4.3 Computational grid for KWU spacer grid

The computational grid has been created using the ANSYS ICEM 11.0 package. The whole domain has been discretized with tetrahedral elements; a prism layer has been added on the walls of the spacer and of the fuel rods, in order to improve the turbulence treatment close to the walls [3]. An overview of the mesh is shown in Figure 8 – a, while a cross section is shown in Figure 8 – b.

To summarize, the mesh of the KWU spacer grid is constituted by 2.7 million of nodes and 9.3 million of cells.

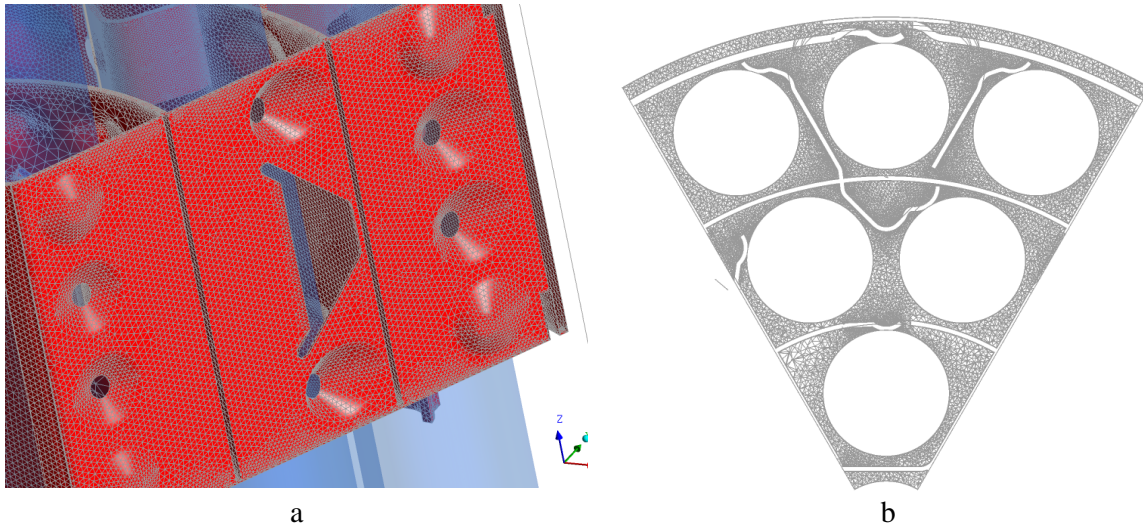


Figure 8. KWU computational grid

### 4.4 Computational grid for IEC spacer grid

The mesh developed for each sector is made of tetrahedral elements, with prisms layers at the walls. The mesh of the sector 1 is constituted by 5.6 million of nodes and 18.2 million of cells.

### 4.5 Set-up of CFD Simulations

Steady state, single phase CFD analyses were conducted by using ANSYS CFX 11.0. All calculations, for both types of spacer grids (i.e KWU and IEC) were set-up according to the following operation conditions:

- Working fluid: Heavy water ( $D_2O$ )
- Temperature: 250 °C (with little differences from case to case)
- Mass flowrate:  $\sim 26$  kg/s (with little differences from case to case)

The reference turbulence model adopted is the Shear Stress Transport (SST) model [4]. The Log-like wall functions available in CFX are used for turbulence near-wall treatment. Sensitivity analyses using different models were performed.

Reference calculations were run using the High Resolution (HR) advection scheme (i.e. the highest order scheme available in CFX). Sensitivity calculations were run using the first-order Upwind (UW) scheme instead.

A no-slip condition was imposed at the walls, with log-law approach for near wall turbulence treatment; i.e. the wall roughness is neglected. In fact, the surface roughness is for this case approximately  $10^{-5}$ ; according to the Moody diagram, for the Reynolds number involved, such value

would increase the friction factor by only a few percents with respect to the smooth pipe case; hence the effect of wall roughness gives a negligible contribution to the overall pressure drop.

Regarding the inlet and outlet boundary conditions, the assumption is made that the spacer is preceded and followed by another spacer, the distance between two successive spacers being 0.455 m.

Considering an indefinite number of successive equidistant spacers, the flow field between spacers  $n$  and  $n+1$  can be expected the same as between spacers  $n-1$  and  $n$ , if no temperature variation occurs (i.e. no heat transfer is present). Therefore, a “periodic” flow configuration takes place, and this must be considered when defining the boundary conditions.

With CFX code, the periodicity can be handled with either of the following two approaches:

1. Iterative process:

- Step 0: calculation with flowrate imposed at inlet, arbitrary velocity and turbulence profiles at inlet; pressure-controlled condition at outlet
- ...
- Step  $k$ : calculation where the outlet velocity and turbulence profiles exported from Step  $k-1$  are imposed as inlet boundary conditions

2. Single periodic calculation:

The outlet and the inlet boundaries are handled as coupled interfaces, so that velocity and turbulence profiles on both of them are forced to be equal. Mass flowrate is imposed.

Sensitivity calculations imposing the single periodic calculation were performed.

## 5 CFD RESULTS FOR KWU SPACER GRID

### 5.1 Summary of results

As reported in Table 1 the reference measured pressure loss coefficient ( $k$ ) is 1.63.

The main features and the results of the calculations are summarized in Table 3, as well as the comparison with the experimental value. Reference calculation is the #14. The best result is given adopting the Upwind advection scheme, the worse one imposing a wall roughness of 16  $\mu$ . It is important to remember that the simulation regard only a 1/6 of the wall domain; in particular it has been chosen, the part of the spacer grid (i.e. the one with the presence of the elastic shoe) that should obstruct more the flow transit with respect to the other part of the domain.

#	Fluid	Turb. model	Adv. scheme	Periodicity	K	(K-Kexp) /Kexp
14Ref	D <sub>2</sub> O	SST	HR	Y	1.40	-14.11%
15	D <sub>2</sub> O	SST	UW	Y	1.63	0.00%
16	D <sub>2</sub> O	SST	HR	N	1.45	-11.04%
17	D <sub>2</sub> O	SST	UW	N	1.66	1.84%
18	D <sub>2</sub> O	SST	HR	N	1.43	-12.27%
19	D <sub>2</sub> O	k-e	UW	N	1.69	3.68%
20	H <sub>2</sub> O	SST	HR	Y	1.39	-14.72%

Table 3 – Summary of the results

### 5.2 Sensitivity calculation

In order to comply as far as possible with the BPG recommendations, some sensitivity calculations have been performed.

Reference calculation was run using the High Resolution (HR) advection scheme. Sensitivity calculations were run using the first-order Upwind (UW) scheme instead. Results are reported in Table 4, and show noticeable influence of the discretization scheme on the results. The adoption of UW yields an increase by 16% of the pressure loss coefficients. The results from the HR scheme are obviously expected to be more accurate than those from UW; on the other hand, the convergence of

HR calculations was lower-quality than for UW calculations (i.e. the residuals could not drop below  $10^{-4}$  with HR, while they could drop below  $10^{-6}$  for with UW).

#	Turb. model	Adv. scheme	Periodicity	K
14Ref	SST	HR	Y	1.40
15	SST	UW	Y	1.63 (+16%)
18	SST	HR	N	1.43
17	SST	UW	N	1.66 (+16%)

Table 4 – Sensitivity to advection scheme

The pressure loss through the spacer is affected by the way the periodicity is dealt with. Results of this sensitivity analysis are reported in Table 5. The reference case involved the iterative process, which tends to a flow configuration where the outlet velocity and turbulence profiles fit with the inlet profiles (periodicity condition). The second calculation was run without accounting for the periodicity at all; uniform velocity and turbulence profiles are imposed at the inlet boundary, while the average pressure is imposed at the outlet boundary ( $p=0$ ).

What can be deduced from the Table is that deviations from the postulated periodicity condition (infinite number of equidistant spacers) can induce increases of the pressure loss coefficient up to 4%.

#	Turb. model	Adv. scheme	Periodicity	K
14Ref	SST	HR	Y	1.40
16	SST	HR	N	1.45 (+4%)

Table 5 – Sensitivity to advection scheme

The sensitivity analysis on working fluid seems not to put in evidence the influence of a different value of the fluid properties; in fact, as reported in Table 6, the K value for the H2O case is very close to the D2O case (difference less than 1%).

#	Fluid	Turb. model	Adv. scheme	Periodicity	K
14Ref	D2O	SST	HR	Y	1.40
20	H2O	SST	HR	Y	1.39 (-1%)

Table 6 – Sensitivity to working fluid

Two calculations were run not using the periodicity, both with UW advection scheme; k-ε model predicts little higher pressure drops (2%) than SST (see Table 7).

#	Turb. model	Adv. scheme	Periodicity	K
17	SST	UW	N	1.66
19	k-ε	UW	N	1.69 (+2%)

Table 7 – Sensitivity to turbulent model

## 6 CFD RESULTS FOR IEC SPACER GRID

Also for the simulation of the IEC spacer grid the results are reported in terms of pressure loss coefficient related to one single spacer. The pressure loss coefficient is calculated using the Equation 2.

Under certain assumptions, the results for the two sectors can be combined to estimate the pressure loss coefficient for the entire FA cross section. In fact, if the coefficient associated with the  $i$ -th sector is  $K_i$ , and the flow area is  $A_i$ , then the overall pressure loss coefficient is given by:

$$K = \frac{A^2}{\left[ \sum_i \frac{A_i}{\sqrt{K_i}} \right]^2} \quad (3)$$

This relation is obtained imposing the same pressure difference across all sectors. Then we get:

$$K = \frac{A^2}{\left[ 2 \cdot \frac{A_1}{\sqrt{K_1}} + 2 \cdot \frac{A_2}{\sqrt{K_2}} + 2 \cdot \frac{A_3}{\sqrt{K_3}} \right]^2} \quad (4)$$

It has to be considered that the results presented in the following include the contribution of the friction losses along the coolant channel to the overall pressure loss.

## 6.1 Summary of results

The main features and the results of the calculations addressed in this report are summarized in Table 8. The cases from 21 to 36 are related to the sector 1; the cases 37 and 38 are related to the sector 2 and to the sector 3 respectively.

#	Grid	Sector	Flow rate [kg/s]	Adv. scheme	Turb. model	Perio	Solver	Temp [K]	K
22	IEC extruded	1	27	UW	SST	N	SS	278	2.67
23	IEC	1	0.1	UW	SST	N	SS	278	5.00
24	IEC	1	1	UW	SST	N	SS	278	2.68
25	IEC	1	10	UW	SST	N	SS	278	2.32
26	IEC	1	27	UW	SST	N	SS	278	2.24
27	IEC	1	100	UW	SST	N	SS	278	2.17
28	IEC	1	27	UW	SST	N	SS	313	2.23
29	IEC	1	27	UW	SST	Y	TR	278	1.79
30	IEC	1	27	HR	SST	N	SS	278	2.51
31	IEC	1	27	HR	SST	N	TR	278	2.88
32	IEC	1	27	UW	k-e	N	SS	278	2.30
34	IEC extruded	1	27	HR	SST	Y	SS	278	2.48
35	IEC extruded	1	27	HR	SST	Y	TR	278	2.38
36	IEC	1	27	HR	SST	Y	TR	278	3.25
37	IEC	2	27	HR	SST	Y	TR	278	2.57
38	IEC	3	27	HR	SST	Y	TR	278	2.33

Table 8 – Summary of results

The reference cases (three calculations) have the following features:

- Domain: sector 1, sector 2 and sector 3
- Turbulence model: SST
- Advection scheme: High Resolution
- Periodicity: activated

The results of the three calculations (i.e. for each sectors) are reported in Table 9. The pressure loss coefficient for the entire fuel assembly cross section is estimated using Equation 4.

Calc. #	Domain	Pressure loss coeff. (K)
36	Sector 1	3.25
37	Sector 2	2.57
38	Sector 3	2.33
-	<i>Entire cross section</i>	2.68

Table 9 – Reference results

As reported in Table 1, measured pressure loss coefficient is 2.18. The k value obtained with CFD simulation for the entire cross section is compared with the experimental value in Table 10.

Domain	Pressure loss coeff. (K)	(K-Kexp) /Kexp
Entire cross section	2.68	22.94%

Table 10 – Comparison with the experimental data

## 6.2 Sensitivity calculation

Two simulations were performed to evaluate the sensitivity to the turbulent modelling. The use of k-ε turbulent model gives an increase of 2.7 % in term of k factor with respect to the SST turbulent model (see Table 11).

Run ID	Grid ID	Turbulent Model	K
26	IEC	SST	2.24
32	IEC	k-ε	2.30 (+2.7%)

Table 11 – Sensitivity to turbulence model

Reference calculation was run using the High Resolution advection scheme; sensitivity calculation was run using the first-order Upwind (UW) scheme instead. Results are reported in Table 12, and show noticeable influence of the discretization scheme on the results. The adoption of UW yields an increase by 12% of the pressure loss coefficients.

Run ID	Grid ID	Advection Scheme	K
26	IEC	Upwind	2.24
30	IEC	High Res.	2.51 (+12%)

Table 12 – Sensitivity to advection scheme

A different position of the inlet and outlet boundary conditions (see Figure 9) was taken into account in order to consider the effect due to the distributed pressure drop.

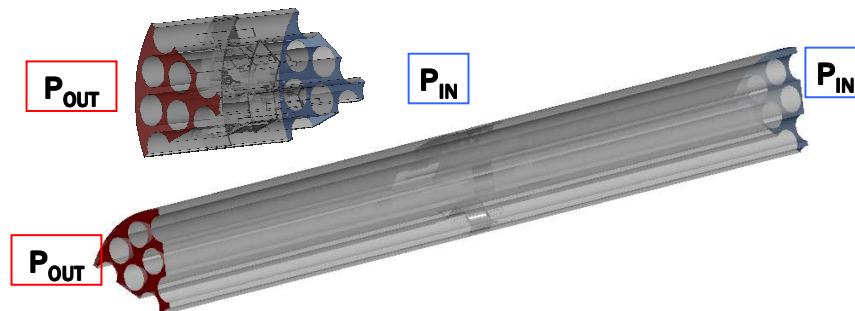


Figure 9. IEC boundary position

The calculation with the extruded domain yields an increase by 12% of the pressure loss coefficients, as reported in Table 13.

Run ID	Grid ID	Extruded	K
26	IEC	N	2.24
22	IEC	Y.	2.67 (+19%)

Table 13 – Sensitivity to boundaries position

The pressure loss through the spacer is affected by the way the periodicity is dealt with. Results of this sensitivity analysis are reported in Table 14. The periodicity condition (infinite number of equidistant spacers) can induce a decrease of the pressure loss coefficient up to 20%.

Run ID	Grid ID	Periodicity	K
26	IEC	N	2.24
29	IEC	Y.	1.79 (-20%)

Table 14 – Sensitivity to periodicity

Different mass flow rates have been taken into account; Figure 10 shows how the K factor is affected by the velocity.

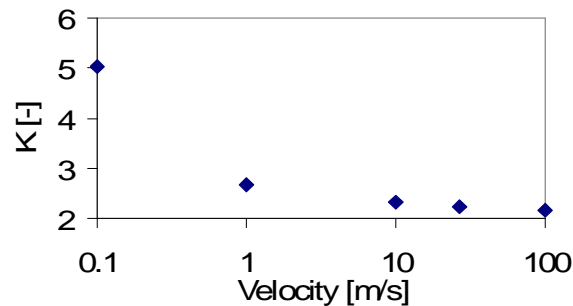


Figure 10. Dependence on mass flow rate

In Table 15 the dependence of the pressure drop for different value of mass flow rate is reported.

Run ID	Grid ID	Mass Flow Rate [Kg/s]	K
23	CNA2	0.1	5.02
24	CNA2	1	2.68
25	CNA2	10	2.32
26	CNA2	27	2.24
27	CNA2	100	2.17

Table 15 – Dependence on mass flow rate

The reference calculation has been simulated considering the spacer grid at the inlet zone of the coolant channel where the temperature is 278° C. A sensitivity calculation has been made considering the spacer grid at the outlet zone of the coolant channel and imposing a temperature of 313° C. The increase of the temperature entails a decrease of the pressure drop (see Table 16).

Run ID	Grid ID	Temperature [°C]	K
26	IEC	278	2.24
28	IEC	313	2.23 (-0.4%)

Table 16 – Sensitivity to temperature

## 7 CONCLUSIONS

CFD simulations of spacer grids of Atucha-II coolant channel were presented. The aim was to contribute to the qualification of the proposed CFD modelling approach for predicting the pressure drops along the channel during the normal operation. Two different spacer grids (namely KWU and IEC) were simulated using the ANSYS CFX 11 package.

Several sensitivity analyses (e.g. sensitivity to turbulent model, advection scheme, working fluid, etc.) were performed for the KWU and IEC spacer grids, in compliance with the BPG recommendations. A comparison with the experimental data was made. If the KWU results are in good agreement with the experimental value, the IEC results are improvable particularly changing the advection scheme; for this type of problem the use of upwind (i.e. the first-order scheme) advection scheme seems to yield better results with respect to the high resolution advection scheme.

## **REFERENCES**

1. Hernández, “Ensaio de pérdida de carga en EECC prototipos Atucha II “, 15 August 2008
2. Mahaffy J. et al., “Best practice guidelines for the use of CFD in nuclear reactor safety applications” NEA/CSNI/R(2007)5, April 2007
3. ANSYS ICEM 11.0 User manual
4. ANSYS CFX 11.0 User manual